Journal of Materials Chemistry C

Accepted Manuscript

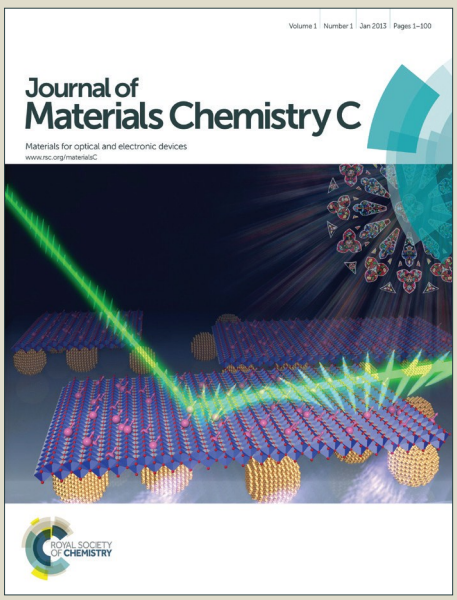

ROYAL SOCIETY OF CHEMISTRY

www.rsc.org/materialsC

Journal of Materials Chemistry C

COMMUNICATION

Low residual donor concentration and enhanced charge transport in low-cost electrodeposited ZnO

Received 00th January 20xx,
Accepted 00th January 20xx

DOI: 10.1039/x0xx00000x

www.rsc.org/

Mourad Benlamri,[a] Samira Farsinezhad,[a] Douglas W. Barlage[a] and Karthik Shankar*[ab]

High unintentional n-type doping and poor charge transport are key limitations in solution processed ZnO thin films. In this context, we report ZnO films with a low residual donor concentration and high texture, synthesized by low-cost electrodeposition on copper. They possess an equilibrium free electron concentration of ~ 2.8 × 10^{14} cm^{-3} and a minimum electron mobility of 80 cm^2 V^{-1} s^{-1}. The resulting Schottky diodes demonstrate rectification ratios of ~ 10^6, ideality factors of ~ 2, and low on-state resistance.

Sol-gel-based growth processes such as spin-coating, doctor blading, and spray pyrolysis attempt to leverage the solution processability of zinc oxide (ZnO) in the service of low-cost mass-producible, roll-to-roll manufacturing-compatible optoelectronic devices, such as photodetectors,[1-3] ultraviolet light-emitting diodes,[4, 5] Schottky diodes,[6] power devices,[7] and thin film transistors for displays.[8] Impressive improvements in the electron mobility of ZnO films grown by these methods have been reported.[9, 10] However, the requirement for a high temperature (400 °C-600 °C) precursor pyrolysis step limits the use of flexible polymeric substrates in general, complicates the process flow, and increases the thermal budget. Although there exist now a number of available methods to convert precursor to stable ZnO film via low-temperature processes, the trade-off is that device performance is generally poorer due to the lower quality of the resulting films.[8]

In this work, we use a distinctly simple, low-cost, low-temperature electrodeposition process, carried out in an atmospheric ambient, to synthesize highly-textured ZnO films optimized for electronic performance with low carrier concentration and high electron mobility. No alloying, doping, annealing, stirring, or vacuum conditions were applied. Electrodeposition of crystalline ZnO thin films from aqueous solutions has been reported independently by Izaki et al.[11] and Peulon et al.[12] in 1996, using nitrate ions and dissolved oxygen as the oxygen precursor, respectively. Pauporté et al.[13] have later demonstrated heteroepitaxial film growth on a single crystalline gallium nitride (GaN) substrate. Electrical characterization of our ZnO films electrodeposited on copper substrates, described in the forthcoming text, revealed a remarkably low carrier concentration of ~ 2.8 × 10^{14} cm^{-3} and a minimum electron mobility of 80 cm^2 V^{-1} s^{-1}. These combined results of carrier concentration and charge transport are close to those obtained in hydrothermally-grown single crystals of bulk ZnO[14] and far superior to those obtained in sol-gel ZnO films.[15-17] Electrodeposition performed at or near the Nernst potential is closer to equilibrium that the highly non-equilibrium kinetically-limited sol-gel process (involving spin-coating and pyrolysis steps),[18-19] and we believe this to be at least partly responsible for the superior structure and composition in electrodeposited ZnO films. Using our electrodeposited ZnO on copper (Cu) substrate, we were able to produce high performance Schottky diodes, meant for extracting carrier concentration and carrier mobility, where the copper growth substrate acts as the barrier metal. These diodes exhibited high rectification ratios of ~ 10^6, low resistance in the on-state, reverse saturation current densities as low as 8 × 10^{-10} A cm^{-2}, and ideality factors as low as 2, in spite of non-optimized ohmic contacts. This set of performance parameters compares very favorably with the current state-of-the-art for Schottky diodes utilizing solution-processed ZnO thin films.[20]

By employing the cathodic electrodeposition method, ZnO films were grown on Cu thin films deposited by the DC magnetron sputtering technique. Commercial fluorine-doped tin oxide (FTO) coatings on glass were also utilized as growth substrates for comparison. The electrolytic solution consisted of 100 mM zinc nitrate hexahydrate (99%, Sigma-Aldrich) dissolved in deionized water. The initial solution pH was 5.2 ± 0.2. The sputtered copper film forming the growth substrate was deposited in one step on a sputtered thin film of titanium tungsten (TiW) which acts as an adhesion and etch-stop layer for diode device processing. The underlying substrate consists

[a] Department of Electrical and Computer Engineering, University of Alberta, Edmonton, AB T6G 2V4, Canada. E-mail: kshankar@ualberta.ca
[b] National Institute for Nanotechnology, National Research Council, 11421 Saskatchewan Drive, Edmonton, AB T6G 2M9, Canada.
Electronic Supplementary Information (ESI) available: Additional electron micro-graphs, absorption and PL spectra of ZnO films. See DOI: 10.1039/x0xx00000x

of commercially supplied wafers of thick silicon oxide (SiO_2) on n-type silicon (*n*-Si).

The deposition mechanism of ZnO film from the zinc nitrate $Zn(NO_3)_2$ precursor in aqueous solution is believed to occur as follows:[21]

$$Zn(NO_3)_2 \rightarrow Zn^{2+} + 2\ NO_3^-$$
$$NO_3^- + H_2O + 2\ e^- \rightarrow NO_2^- + 2\ OH^-$$
$$Zn^{2+} + 2\ OH^- \rightarrow Zn(OH)_2$$
$$Zn(OH)_2 \rightarrow ZnO + H_2O$$

In this work, the electrodeposition potential and temperature conditions were set as to achieve the highest current rectification ratios of the fabricated Schottky diodes. It was found that the most optimal values for the potential ranged between 850 mV and 900 mV for temperatures fixed at values between 80 °C and 85 °C. Under these applied electrodeposition conditions, surface activation of the copper film was necessary to achieve good adhesion at the Cu/ZnO interface. To that effect, we submitted the copper surface to a soft oxygen plasma treatment for a 5 s duration prior to electrodeposition. As a result of contamination removal and surface activation, good interface adhesion was achieved for all applied electrodeposition conditions.

ZnO film electrodeposition on the pretreated copper surface was carried out potentiostatically using a standard three-electrode cell configuration in a glass beaker. The reference electrode consisted of a standard Ag/AgCl electrode (+200 mV vs the standard hydrogen electrode) whereas a deposited platinum (Pt) film and the pretreated copper substrate were set up as counter electrode and working electrode respectively. A computer-controlled CHI660E electrochemical workstation was used to apply potential and record current-time and charge-time data. For both Cu and FTO substrates, electrodeposition was conducted for 15 min at a fixed cathodic potential E_V of -875 mV and a solution temperature of 85 ± 2 °C with no stirring. The total charge registered during deposition was about -5.7 C cm^{-2}, corresponding to a thickness of 5700 ± 20 nm measured by cross-sectional field-emission scanning electron microscopy (FESEM).

The investigation of the surface morphology of the ZnO films electrodeposited on copper by the FESEM imaging technique, presented in Fig. 1a (higher magnification image in Fig. S1 in ESI†), reveals a fully continuous film and a much smoother surface than that obtained, under similar growth conditions, in ZnO films electrodeposited on the standard FTO substrate, shown as inset in Fig. 1a. In addition, the cross-

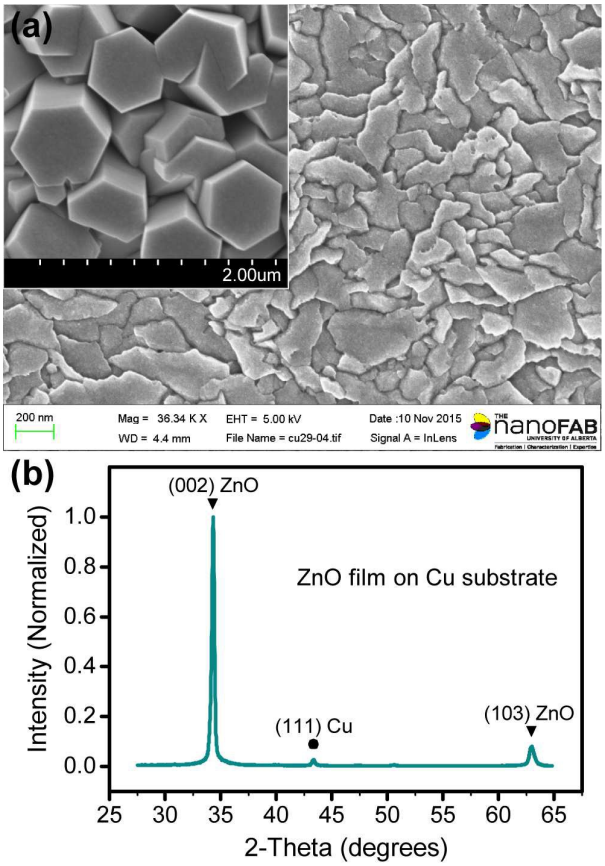

Fig. 1 (a) FESEM images of the surface morphology of electrodeposited ZnO films on Cu (FTO for inset) substrate, and (b) X-ray diffractogram of the same ZnO electrodeposited film on Cu substrate.

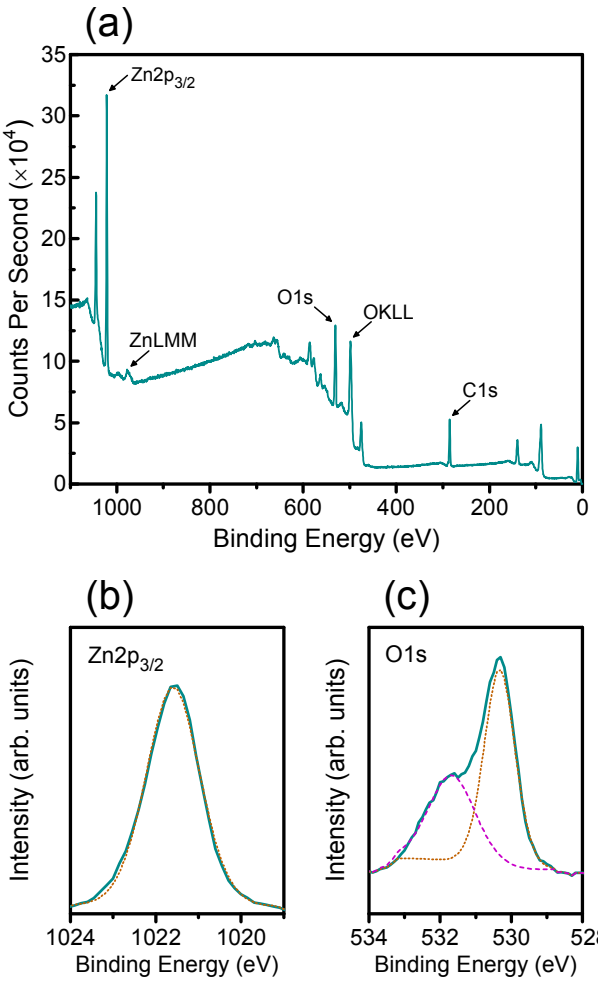

Fig. 2 Recorded survey (a) and high-resolution peak regions spectra for the Zn $2p_{3/2}$ (b) and O 1s (c) photoelectron peaks.

sectional FESEM image (see Fig. S2 in ESI†) of a cleaved Cu/ZnO sample reveals a columnar ZnO film structure.

These observed results were further investigated via the X-ray diffraction (XRD) peak profile, displayed in Fig. 1b, which exhibits a single intense peak, at a diffraction angle $2\theta = 34.33°$, indexed to the (002) Miller planes of hexagonal wurtzite ZnO (PDF card 00-001-1136). This is indicative of a highly preferential crystal orientation in which the c-axis is normal to the substrate. The peak is very narrow with a full-width-at-half-maximum (FWHM) value not exceeding the instrumental peak broadening limit. The calculation of the grain sizes is thus not applicable from the present XRD peak profile but the small FWHM value further attests nonetheless to the large grain sizes nature of the film surface. The ZnO film surface was further investigated by the X-ray photoelectron spectroscopy (XPS) technique with Al Kα radiation (1486.6 eV) as excitation source. Survey and high-resolution peak regions spectra were recorded for the Zn $2p_{3/2}$ and O 1s photoelectron peaks and for the Zn LMM and O KLL Auger peaks as well; they

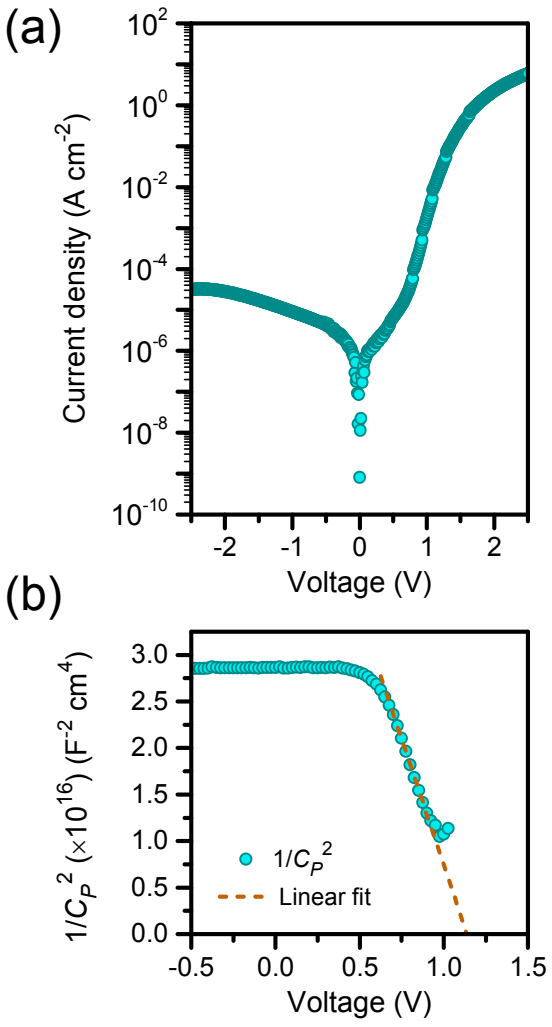

Fig. 3 (a) Room temperature *I-V* characteristics plotted on a semi-log scale, and (b) room temperature $1/C_P^2$-*V* plot taken at 50 kHz with respective linear fit. Both current and capacitance are given per unit area.

are displayed in Fig. 2. Binding energy scale calibration used the C 1s carbon peak at 285 eV as reference. The Zn $2p_{3/2}$ and O 1s photoelectron peaks were recorded at binding energies of 1021.6 ± 0.2 eV and 530.3 ± 0.2 eV respectively. The kinetic energies of the recorded Zn LMM and O KLL Auger peaks were 988.6 ± 0.3 eV and 508.9 ± 0.3 eV respectively. These recorded photoelectron and Auger energies match well with the literature values[22] and confirm the formation of ZnO in the electrodeposited film. The modified Auger parameter α', extracted from the survey data by adding the Zn $2p_{3/2}$ peak binding energy to the Zn $L_3M_{45}M_{45}$ peak kinetic energy, is found to be 2010.2 eV which exactly matches the literature value of bulk ZnO.[22] Because the modified Auger parameter is a good indicator of stoichiometry, we conclude that the ZnO film is stoichiometric even at the surface. We note the presence of a second O 1s peak at 531.7 ± 0.2 eV, acquired from deconvolution of the asymmetric O 1s region, usually attributed to oxygen in surface hydroxyl groups.[23] The O 1s subcomponent peaks usually ascribed to carboneous, carboxylate-type or carbonate-type species on the film surface are not detected, probably as a result of their very low content(s). The percentage atomic concentration of oxygen ascribed to stoichiometric ZnO relative to the whole O 1s peak at the film surface is found to be ~ 61%. It is noteworthy that no nitrogen contamination was detected. The sharp peaks in the room temperature absorption and photoluminescence spectra (Fig. S3 and Fig. S4 respectively in ESI†) indicate the high optical quality of the film.

The fabricated Cu/ZnO/Aluminum (Al) diodes were studied by current-voltage (*I-V*) and capacitance-voltage (*C-V*) measurements performed at room temperature using a Keithley 4200-SCS semiconductor parameter analyzer. The *I-V* characteristics, plotted in Fig. 3a, show excellent rectifying behavior, with a rectification ratio close to 10^6, indicating the formation of a good-quality Schottky barrier at the Cu/ZnO interface. According to thermionic emission theory, the *I-V* relation is given by eqn (1) and eqn (2):

$$I = I_S\left[\exp\left(\frac{q(V - IR_S)}{\eta kT}\right) - 1\right] \quad (1)$$

I_S, the reverse saturation current, is

$$I_S = AA^*T^2\exp\left(\frac{-\phi_B}{kT}\right) \quad (2)$$

where A is the diode area, k the Boltzmann's constant, T the absolute temperature, q the electronic charge, V the applied voltage, Φ_B the Schottky barrier height (SBH), R_S the series resistance, and η the ideality factor. The theoretical value of 32 A cm^{-2} K^{-2} is used for the Richardson's constant A^* by assuming an electron effective mass $m^* \sim 0.27m_0$.[24] The extraction of the ideality factor from the measured ln(*I*)-*V* data was conducted by adopting Cheung's method.[25] From the linear fit of the d*V*/dln(*I*) vs *I* plot, we obtain an ideality factor of 2.04, which compares very favorably with those reported for Schottky contacts made of ZnO films electrodeposited on other metals.[26] It indicates, on the other hand, that the

transport mechanism across the interface is not entirely dominated by thermionic emission, thereby precluding an accurate estimation of the SBH. The measured reverse saturation current density J_S is notably very low with a value of 8×10^{-10} A cm^{-2}. The observed deviation from ideality is due to many factors[27] and, in large part, to the formation on the copper surface of a very thin interfacial layer of copper oxides, generated by unavoidable air oxidation and soft room-temperature oxygen plasma treatment. It is noteworthy that the XRD pattern does not show any diffraction peaks related to Cu_xO_y copper oxides, which supports the assumption that the copper oxides layer would only be a few monolayers thick, not exceeding the native copper oxide layer thickness of ~ 3.2 nm obtained after exposing copper to open air for much longer times.[28] Accordingly, the measured *I-V* data follows a linear dependence for voltages between 0.1 V and 0.4 V indicating that current tunneling and carrier recombination are the dominant contributions to the measured current in this bias regime. Lateral contact inhomogeneities are also expected to contribute significantly to the Schottky barrier nonideality[27] in view of the large circular contact area (radius = 165 μm) of the diode. The series resistance R_S used in eqn (1) can be estimated from the high voltage region of the forward *I-V* characteristics through the relation $\Delta V = R_S \Delta I$.[29] By taking ΔV between 1.75 V and 2.5 V, a value R_S = 182 Ω is obtained. This value is relatively low considering the non-optimized quality of our ZnO/Al ohmic contact. Knowing that the series resistance fraction in the semiconductor $R_{S,SC}$ has to be lower than the diode series resistance R_S ($R_{S,SC}$ < 182 Ω) and using the known device dimensions (Al contact radius = 165 μm and ZnO film thickness = 5700 nm), an upper limit of the ZnO film resistivity was estimated as ρ < 273 Ω cm.

Capacitance-voltage measurements were also carried out at room temperature to determine the free carrier concentration. At a detection signal frequency of 50 kHz, diode capacitance density C_P was measured vs voltage *V* and a plot of $1/C_P^2$ vs *V* data is shown in Fig. 3b. It reveals that the ZnO layer is fully depleted at the zero voltage bias, an indicator of low doping levels in view of the large layer thickness (~ 5700 nm). The fitting of the linearly varying portion of this plot, according to Mott-Schottky analysis, allows extraction of the built-in potential V_{bi} = 1.16 V and free carrier concentration $N = 2.8 \times 10^{14}$ cm^{-3} from eqn (3):[29]

$$N = -\frac{2}{e\varepsilon_S\varepsilon_0}\left[\frac{d}{dV}\left(\frac{1}{C_P^2}\right)\right]^{-1} \qquad (3)$$

where *e* is the electronic charge, ε_S the dielectric constant of ZnO, and ε_0 the vacuum permittivity.

The value of the built-in potential is clearly overestimated as it falls above the range of values reported in the literature.[30] Two commonly known reasons contribute to this discrepancy: 1) the barrier nonparabolicity, due the interfacial oxide shallow layer, leads evidently to an overestimation of V_{bi} by the Mott-Schottky analysis, and 2) in Schottky barriers with lightly doped semiconductors, the measured capacitances are usually very small (< 4 pF in our case) and become prone to errors introduced by small but non negligible excess shunt capacitances,[31] which have the effect of overestimating both V_{bi} and *N*.

In light of the relatively low resistivity (ρ < 273 Ω cm), the low level of unintentional n-type doping, $N = 2.8 \times 10^{14}$ cm^{-3}, achieved in our electrodeposited ZnO is remarkable and is on par with the low carrier concentration values reported in hydrothermally-grown bulk ZnO.[14] Although the origin of the unintentional n-type doping in ZnO is still under debate within the scientific community, it is commonly attributed to native defects and unintentional incorporation of impurities such as hydrogen. A low level of unintentional doping thus indicates a low defect-grown ZnO film. The low values of the estimated ρ and *N* hint at a significantly high electron mobility in the bulk semiconductor. Applying the relations $1/\rho = qN\mu$ and ρ < 273 Ω cm, a low limit of the mobility μ can be assessed: μ > 80 cm^2 V^{-1} s^{-1}. It is noteworthy that The mobility in our ZnO films is expected to be greatly enhanced by the low density of scattering centers and grain boundaries owing to the good film crystalline quality and vertical carrier transport along the (002)-oriented columnar film structure.

Conclusions

In conclusion, we have combined a suitable substrate (copper) with an underutilized low-cost processing technique (electrodeposition) to synthesize ZnO films with extremely low free carrier concentrations and strong crystallographic texture. The underlying copper substrate was found to form an excellent Schottky barrier with the electrodeposited ZnO film. The resulting diodes stood out from previously reported solution-processed ZnO devices in terms of their superior electrical characteristics. Good electron transport in these films was inferred from the ohmic conduction region obtained at high forward bias. These electrodeposited ZnO films are particularly suitable for building large-scale low-cost vertical devices with high breakdown voltage and high current handling capabilities.

Acknowledgements

The authors would like to thank nanoBridge and NSERC for supporting this work and would like to acknowledge CMC Systems for financial assistance relating to microfabrication. The authors would also like to acknowledge the University of Alberta nanoFab for usage of equipment and the Canada Foundation for Innovation (CFI) and the Alberta Small Equipment Research Program (SEGP) for funding of research infrastructure.

Notes and references

1. W. Dai, X. Pan, S. Chen, C. Chen, Z. Wen, H. Zhang and Z. Ye, *J. Mater. Chem. C*, 2014, **2**, 4606-4614.
2. X. Wang, W. Tian, M. Liao, Y. Bando and D. Golberg, *Chem. Soc. Rev.*, 2014, **43**, 1400-1422.

3. X. Liu, L. Gu, Q. Zhang, J. Wu, Y. Long and Z. Fan, *Nat. Commun.*, 2014, **5**, 4007.
4. Q.-J. Feng, H.-W. Liang, Y.-Y. Mei, J.-Y. Liu, C. C. Ling, P.-C. Tao, D.-Z. Pan and Y.-Q. Yang, *J. Mater. Chem. C*, 2015, **3**, 4678-4682.
5. B. R. Lee, E. D. Jung, J. S. Park, Y. S. Nam, S. H. Min, B.-S. Kim, K.-M. Lee, J.-R. Jeong, R. H. Friend, J. S. Kim, S. O. Kim and M. H. Song, *Nat. Commun.*, 2014, **5**, 4840.
6. J. Zhang, Y. Li, B. Zhang, H. Wang, Q. Xin and A. Song, *Nat. Commun.*, 2015, **6**, 7561.
7. Q. Xin, L. Yan, Y. Luo and A. Song, *Appl. Phys. Lett.*, 2015, **106**, 113506.
8. S. R. Thomas, P. Pattanasattayavong and T. D. Anthopoulos, *Chem. Soc. Rev.*, 2013, **42**, 6910-6923.
9. M. Benlamri, K. M. Bothe, A. M. Ma, G. Shoute, A. Afshar, H. Sharma, A. Mohammadpour, M. Gupta, K. C. Cadien, Y. Y. Tsui, K. Shankar and D. W. Barlage, *Phys. Status Solidi-R*, 2014, **8**, 871-875.
10. G. Adamopoulos, S. Thomas, P. H. Wobkenberg, D. D. C. Bradley, M. A. McLachlan and T. D. Anthopoulos, *Adv. Mater.*, 2011, **23**, 1894-1898.
11. M. Izaki and T. Omi, *J. Electrochem. Soc.*, 1996, **143**, L53-L55.
12. S. Peulon and D. Lincot, *Adv. Mater.*, 1996, **8**, 166-170.
13. T. Pauporté and D. Lincot, *Appl. Phys. Lett.*, 1999, **75**, 3817-3819.
14. K. Maeda, M. Sato, I. Niikura and T. Fukuda, *Semicond. Sci. Tech.*, 2005, **20**, S49-S54.
15. A. H. Adl, A. Ma, M. Gupta, M. Benlamri, Y. Y. Tsui, D. W. Barlage and K. Shankar, *ACS Appl. Mater. Interfaces*, 2012, **4**, 1423-1428.
16. A. H. Adl, P. Kar, S. Farsinezhad, H. Sharma and K. Shankar, *RSC Adv.*, 2015, **5**, 87007-87018.
17. R. Ghosh, G. K. Paul and D. Basak, *Mater. Res. Bull.*, 2005, **40**, 1905-1914.
18. B. S. Ong, C. S. Li, Y. N. Li, Y. L. Wu and R. Loutfy, *J. Amer. Chem. Soc.*, 2007, 129, 2750-2751.
19. C. Li, Y. Li, Y. Wu, B. Ong and R. Loutfy, *J. Mater. Chem.*, 2009, **19**, 1626-1634.
20. M. Yilmaz, Z. Caldiran, A. R. Deniz, S. Aydogan, R. Gunturkun and A. Turut, *Appl. Phys. A-Mater.*, 2015, **119**, 547-552.
21. T. Yoshida, D. Komatsu, N. Shimokawa and H. Minoura, *Thin Solid Films*, 2004, **451**, 166-169.
22. J. F. Moulder, W. F. Stickle, P. E. Sobol and K. D. Bomben, *Handbook of X-ray Photoelectron Spectroscopy*, Physical Electronics, Eden Prairie, MN, 1995.
23. G. Ballerini, K. Ogle and M.-G. Barthés-Labrousse, *Appl. Surf. Sci.*, 2007, **253**, 6860-6867.
24. S. M. Sze and K. K. Ng, *Physics of Semiconductor Devices*, John Wiley and Sons, Hoboken, NJ, third edn., 2006.
25. S. K. Cheung and N. W. Cheung, *Appl. Phys. Lett.*, 1986, **49**, 85-87.
26. S. Chatman, B. J. Ryan and K. M. Poduska, *Appl. Phys. Lett.*, 2008, **92**, 012103.
27. R. T. Tung, *Appl. Phys. Rev.*, 2014, **1**, 011304.
28. P. Keil, R. Frahm and D. Lützenkirchen-Hecht, *Corros. Sci.*, 2010, **52**, 1305-1316.
29. D. K. Schroder, *Semiconductor Material and Device Characterization*, John Wiley and Sons, Hoboken, NJ, third edn., 2006.
30. L. J. Brillson and Y. Lu, *J. Appl. Phys.*, 2011, **109**, 121301.
31. P. K. Vasudev, B. L. Mattes, E. Pietras and R. H. Bube, *Solid-State Electron.*, 1976, **19**, 557-559.